PROCEEDINGS OF SCIENCE

Hyperons in nuclear matter studied in chiral effective field theory

Johann Haidenbauer*
Institute for Advanced Simulation, Forschungszentrum Jülich GmbH, D-52428 Jülich, Germany
E-mail: j.haidenbauer@fz-juelich.de

Results of a study of the hyperon-nucleon system within chiral effective field theory are reported. The investigation is based on the scheme proposed by Weinberg which has been applied rather successfully to the nucleon-nucleon interaction in the past. Calculations for the ΛN and ΣN interactions in free space, obtained up to next-to-leading order, are briefly reviewed. In addition the in-medium properties of this YN interaction are considered. Specifically, binding energies of the Λ and Σ hyperons in nuclear matter are presented, based on a conventional first-order Brueckner calculation, and the Λ-nuclear spin-orbit interaction is discussed.

The 8th International Workshop on Chiral Dynamics
29 June 2015 - 03 July 2015
Pisa, Italy

*Speaker.

PoS(CD15)106

1. Introduction

Chiral effective field theory (EFT) as proposed in the pioneering works of Weinberg [1] is a powerful tool for the derivation of baryonic forces. In this scheme there is an underlying power counting which allows to improve calculations systematically by going to higher orders in a perturbative expansion. In addition, it is possible to derive two- and corresponding three-body forces as well as external current operators in a consistent way.

Recently, a hyperon-nucleon (YN) interaction has been derived up to next-to-leading order (NLO) in chiral EFT by the Jülich-Bonn-Munich group [2]. At that order there are contributions from one- and two-pseudoscalar-meson exchange diagrams and from four-baryon contact terms without and with two derivatives. SU(3) flavor symmetry is imposed for constructing the YN interaction in order to reduce the number of free parameters, in particular the number of low-energy constants (LECs) associated with the arising contact terms. In the actual calculation the SU(3) symmetry is broken, however, by the mass differences between the involved mesons (π, K, η) and between the baryons (N, Λ, Σ). An excellent description of available ΛN and ΣN scattering data could be achieved at NLO [2].

The YN interaction is an important ingredient for microscopic calculations of hypernuclei and it is also relevant for understanding the physics of neutron stars. Motivated by these aspects we examine the in-medium properties of the YN interaction derived within chiral EFT [3, 4]. In particular, the single-particle potentials for the Λ and Σ hyperons in nuclear matter are evaluated in a conventional G-matrix calculation, and the Scheerbaum factor [5] associated with the hyperon-nucleus spin-orbit interaction is computed. One issue of special interest is the Σ-nucleus potential. There is strong phenomenological evidence that it is repulsive [6]. However, microscopic models of the YN interaction, fitted to ΛN and ΣN scattering data, often fail to produce a repulsive Σ-nuclear potential. Specifically, for models based on meson-exchange dynamics it is rather difficult to obtain such a repulsion [7].

Another issue of interest is the Λ-nucleus spin-orbit interaction where empirical information suggests that it should be rather weak [8, 9, 10]. Therefore, we investigate also the spin-orbit interaction and, in particular, the role of the antisymmetric spin-orbit force in the YN system. As mentioned above, the chiral EFT approach yields a potential that contains, besides pseudoscalar meson exchanges, a series of contact interactions with an increasing number of derivatives. In this approach a contact term representing an antisymmetric spin-orbit force arises already at NLO. It induces ${}^1P_1$–${}^3P_1$ transitions in the coupled (isospin $I = 1/2$) ΛN–ΣN system. The low-energy constant associated with the contact term could not be pinned down by a fit to the existing ΛN and ΣN scattering data as found in Ref. [2] and, thus, it was simply put to zero in that work. However, its value can be fixed from investigating the properties of the Λ hyperon in nuclear matter and, specifically, it can be utilized to achieve a weak Λ-nuclear spin-orbit potential [3, 4].

2. The YN interaction in chiral EFT

The derivation of the chiral baryon-baryon potentials for the strangeness sector at leading order (LO) using the Weinberg power counting is outlined in Refs. [11, 12]. Details for the NLO case can be found in Ref. [2], see also [13]. The LO potential consists of four-baryon contact

terms without derivatives and of one-pseudoscalar-meson exchanges while at NLO contact terms with two derivatives arise, together with contributions from (irreducible) two-pseudoscalar-meson exchanges. The contributions from pseudoscalar-meson exchanges (π, η, K) are completely fixed by the assumed SU(3) flavor symmetry. On the other hand, the strength parameters associated with the contact terms, the LECs, need to be determined in a fit to data. How this is done is described in detail in Ref. [2]. Note that we impose also SU(3) symmetry for those contact terms which reduces the number of independent LECs that can contribute.

The reaction amplitudes are obtained from the solution of a coupled-channels Lippmann-Schwinger (LS) equation for the derived interaction potentials:

$$T^{\rho''\rho',J}_{\nu''\nu'}(p'',p';\sqrt{s}) = V^{\rho''\rho',J}_{\nu''\nu'}(p'',p') + \sum_{\rho,\nu}\int_0^\infty \frac{dpp^2}{(2\pi)^3} V^{\rho''\rho,J}_{\nu''\nu}(p'',p)\frac{2\mu_\nu}{q^2_\nu - p^2 + i\eta} T^{\rho\rho',J}_{\nu\nu',J}(p,p';\sqrt{s}) \; .$$

The label ν indicates the particle channels and the label ρ the partial wave. μ_ν is the pertinent reduced mass. The on-shell momentum in the intermediate state, q_ν, is defined by $\sqrt{s} = \sqrt{m^2_{B_{1,\nu}} + q^2_\nu} + \sqrt{m^2_{B_{2,\nu}} + q^2_\nu}$. Relativistic kinematics is used for relating the laboratory energy $T_{\rm lab}$ of the hyperons to the c.m. momentum.

We solve the LS equation in the particle basis, in order to incorporate the correct physical thresholds. Depending on the total charge, up to three baryon-baryon channels can couple. The Coulomb interaction is taken into account appropriately via the Vincent-Phatak method [14]. The potentials in the LS equation are cut off with a regulator function, $f_R(\Lambda) = \exp\left[-\left(p'^4 + p^4\right)/\Lambda^4\right]$, in order to remove high-energy components [15]. We consider cutoff values in the range $\Lambda = 550$ – 700 MeV (LO) and $\Lambda = 500$ – 650 MeV (NLO), similar to what was used for chiral NN potentials [15].

3. Results for ΛN and ΣN in free space

Our results for ΛN and ΣN scattering are presented in Fig. 1. The bands (red for NLO and green for LO) represent the variation of the cross sections based on chiral EFT within the considered cutoff region, i.e. 550-700 MeV in the LO case [11] and 500-650 MeV at NLO. For comparison also results for the Jülich '04 [16] meson-exchange model are shown (dashed line).

Obviously, the available ΛN and ΣN scattering data are very well described by our NLO EFT interaction. In particular, and as expected, the energy dependence exhibited by the data is visibly better reproduced within our NLO calculation than at LO. This concerns especially the $\Sigma^+ p$ channel. But also for Λp the NLO results are now well in line with the data even up to the ΣN threshold. Furthermore, one can see that the dependence on the cutoff mass is strongly reduced in the NLO case. Additional results, for differential cross sections and for phase shifts, can be found in Ref. [2].

Besides an excellent description of the YN data the chiral EFT interaction yields a satisfactory value for the hypertriton binding energy, see Ref. [2]. Calculations for the four-body hypernuclei ${}^4_\Lambda$H and ${}^4_\Lambda$He based on the EFT interactions can be found in Ref. [17].

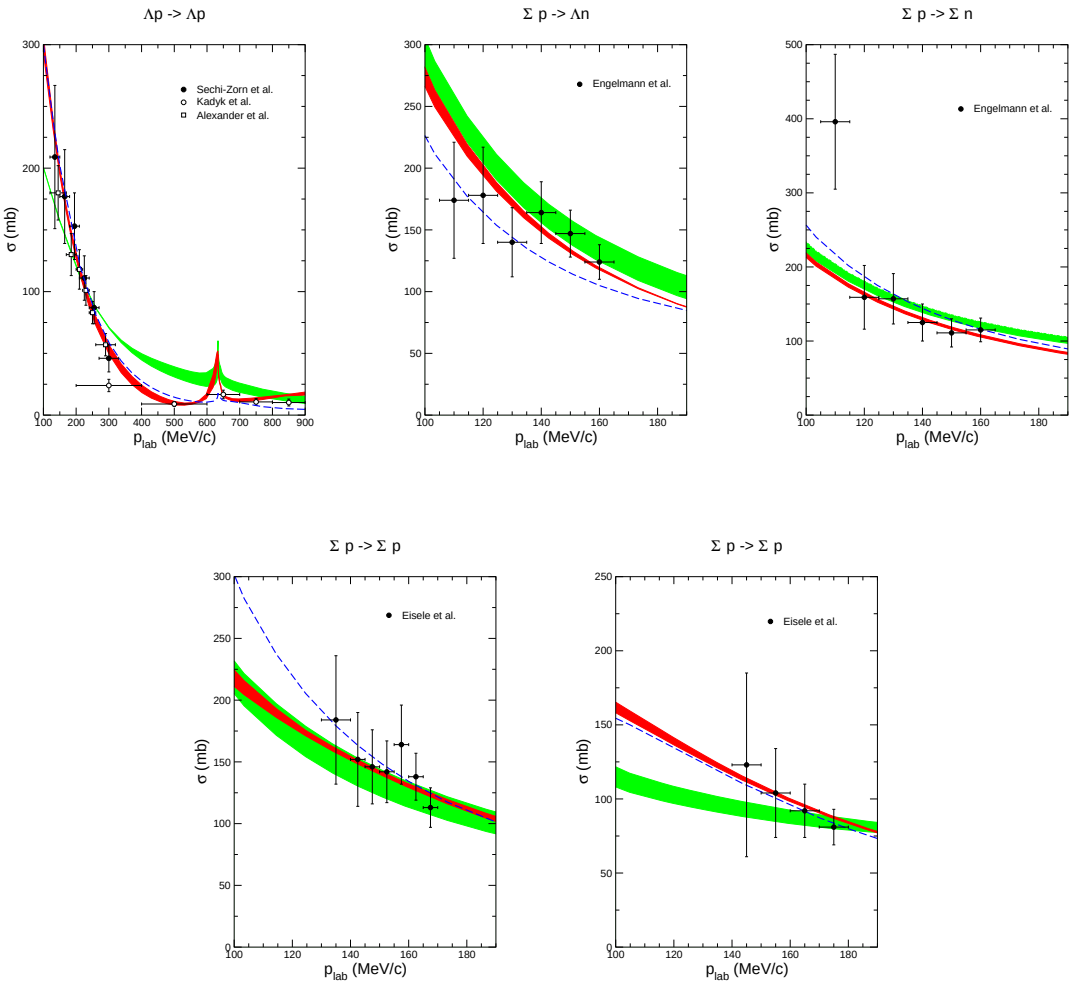

Figure 1: Total cross sections for ΛN and ΣN scattering as a function of the laboratory momentum p_{lab}. The green band shows the chiral EFT results to LO for variations of the cut-off in the range $\Lambda = 550$–700 MeV, while the red band are results to NLO for $\Lambda = 500$–650 MeV. The dashed curve is the result of the Jülich '04 [16] meson-exchange potential.

4. Results for the Λ and Σ in nuclear matter

Recently, we investigated also the properties of our YN interactions in nuclear matter [3, 4]. Specifically, we performed conventional first-order Brueckner calculations based on the standard (gap) choice of the single-particle (s.p.) potentials [3] as well as with the continuous choice [4]. In the present work we focus on the results of Ref. [3].

Starting point of our nuclear matter calculation is the Bethe-Goldstone equation

$$\langle YN|G_{YN}(\zeta)|YN\rangle = \langle YN|V|YN\rangle$$

$$+ \sum_{Y'N} \langle YN|V|Y'N\rangle \, \langle Y'N|\frac{Q}{\zeta - H_0}|Y'N\rangle \, \langle Y'N|G_{YN}(\zeta)|YN\rangle \, , \qquad (4.1)$$

which defines the YN reaction matrix G_{YN}. Here, Q denotes the Pauli projection operator, which excludes those intermediate YN states with the nucleon inside the Fermi sea. The starting energy ζ in the Bethe-Goldstone equation (4.1) is defined by

$$\zeta = E_Y(p_Y) + E_N(p_N) \, , \qquad (4.2)$$

where the single particle energies of the baryons are given by

$$E_\alpha(p_\alpha) = M_\alpha + \frac{p_\alpha^2}{2M_\alpha} + U_\alpha(p_\alpha), \qquad \alpha = Y, \, N, \qquad (4.3)$$

i.e. these include the (nonrelativistic) kinetic energy and the baryon mass, and also the s.p. potential U_α. The nucleon s.p. potential U_N is taken from a separate calculation of pure nuclear matter based on a phenomenological NN potential, see the comment in Ref. [3], while the s.p. potential of the hyperons is calculated via

$$U_Y(p_Y) = \int_{p_N \le k_F} d^3p_N \, \langle YN|G_{YN}(\zeta(U_Y))|YN\rangle \, , \qquad (4.4)$$

which means that it is determined self-consistently with Eq. (4.1) in the standard way. k_F is the Fermi momentum which is related to the nuclear matter density ρ via $\rho = (2/3\pi^2)k_F^3$. Finally, in lowest order in the so-called hole-line expansion [18], to which we restrict ourselves here, the binding energy of a hyperon in infinite nuclear matter is given by $B_Y(\infty) = -U_Y(p_Y = 0)$, evaluated at the saturation point of nuclear matter.

The strength of the s.p. spin-orbit potential of a hyperon in nuclear matter is most conveniently quantified by the so-called Scheerbaum factor S_Y [5], which is defined by [19]

$$U_\Lambda^{\ell s}(r) = -\frac{\pi}{2} S_Y \frac{1}{r}\frac{d\rho(r)}{dr} \ell \cdot \sigma \, . \qquad (4.5)$$

Here $\rho(r)$ is the nucleon density distribution and ℓ the single-particle orbital angular momentum operator. The quantity S_Y can be expressed in terms of the (partial-wave projected) G-matrix elements in the form

$$\begin{aligned} S_Y(p_Y) \, = \, & - \frac{3\pi}{4(k_F)^3} \, \xi_Y(1+\xi_Y)^2 \sum_{I_0,J} \frac{2I_0+1}{(2I_Y+1)}(2J+1) \\ & \int_0^{p_{max}} \frac{d\,p}{(2\pi)^3} \, W(p,p_Y) \, \Big\{ \, (J+2)\, G^{J,I_0}_{Y1J+1,Y1J+1}(p,p;p_Y) \\ & + G^{J,I_0}_{Y1J,Y1J}(p,p;p_Y) - (J-1)\, G^{J,I_0}_{Y1J-1,Y1J-1}(p,p;p_Y) \\ & - \sqrt{J(J+1)} \, \Big[\, G^{J,I_0}_{Y1J,Y0J}(p,p;p_Y) + G^{J,I_0}_{Y0J,Y1J}(p,p;p_Y) \Big] \Big\} \, , \end{aligned} \qquad (4.6)$$

with $G^{J,I_0}_{YSL,Y'S'L'}$ being the matrix element for a specific total angular momentum J and isospin I_0 and outgoing and incoming spins (S, S') and orbital angular momenta (L, L'). The explicit expression for the weight function $W(p,p_Y)$ can be found in Ref. [3], together with a more detailed description of the formalism. ξ_Y denotes the mass ratio, $\xi_Y = M_N/M_Y$.

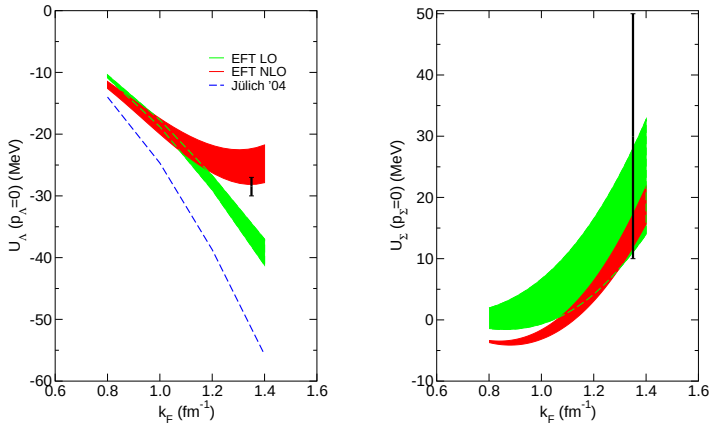

Figure 2: The Λ and Σ s.p. potentials, $U_\Lambda(p_\Lambda = 0)$ and $U_\Sigma(p_\Sigma = 0)$, as a function of the Fermi momentum k_F. The green band shows the chiral EFT results to LO for variations of the cut-off in the range $\Lambda = 550$–700 MeV, while the red band are results to NLO for $\Lambda = 500$–650 MeV. The dashed curve is the result of the Jülich '04 [16] meson-exchange potential. The vertical lines indicate the "empirical" range taken from Ref. [9].

Let us now come to the results. Table 1 summarizes the values for the Λ and Σ potential depths, $U_\Lambda(p_\Lambda = 0)$ and $U_\Sigma(p_\Sigma = 0)$, evaluated at the saturation point of nuclear matter, i.e. for $k_F = 1.35$ fm^{-1}. Corresponding results obtained for the Jülich meson-exchange potentials from 2004 [16] and 1994 [20] are also included. In case of the EFT interactions we show the variation with the cutoff. These are comparable for U_Λ at LO and NLO, but noticeably reduced for U_Σ at NLO. The dependence of the hyperon potential depths on the Fermi momentum is displayed in Fig. 2.

The predictions for $U_\Lambda(0)$ at NLO, for nuclear matter saturation density as given in Table 1, are well in line with the 'empirical' value for the Λ binding energy in nuclear matter of about -27 to -30 MeV, deduced from the binding energies of finite Λ hypernuclei [21].

Table 1: Results for the s.p. potentials $U_\Lambda(0)$ and $U_\Sigma(0)$ (in MeV) based on our EFT potentials and the Jülich meson-exchange interactions.

	EFT LO	EFT NLO	Jülich '04 [16]	Jülich '94 [20]
Λ [MeV]	$550 \cdots 700$	$500 \cdots 650$		
$U_\Lambda(0)$	$-38.0 \cdots -34.4$	$-28.2 \cdots -22.4$	-51.2	-29.8
$U_\Sigma(0)$	$28.0 \cdots 11.1$	$17.3 \cdots 11.9$	-22.2	-71.4

The predicted Σ s.p. potential is repulsive (at NLO and also at LO), see Table 1. As already mentioned in the Introduction, this result is in agreement with evidence from the analysis of level shifts and widths of Σ^- atoms and from recently measured (π^-, K^+) inclusive spectra related to Σ^--formation in heavy nuclei [22, 23]. We could achieve a repulsive Σ s. p. potential because

the interaction in the ${}^3S_1$ partial wave of the $\Sigma^+ p$ channel (which provides the dominant contribution, cf. Table 4 in [3]) is repulsive, for the LO potential but also for the NLO interaction. Note, however, that with regard to the NLO interaction it had turned out that, in principle, the available YN scattering data can be fitted equally well with an attractive or a repulsive interaction in the ${}^3S_1$ partial wave of the $I = 3/2$ ΣN channel [2]. The repulsive solution was adopted for the reasons just discussed, but also in accordance with results from a first lattice QCD calculation [24]. As exemplified by the predictions of the Jülich meson-exchange models, typically such phenomenological potentials fail to produce a repulsive Σ-nuclear potential. For exceptions see Ref. [7].

Results for the Scheerbaum factor S_Λ that characterizes the strength of the Λ-nuclear spin-orbit potential in nuclear matter, see Eq. (4.5), are provided in Table 2. While the results at LO are pure predictions, those at NLO depend on a LEC that generates ${}^1P_1$–${}^3P_1$ transitions in the coupled ($I = 1/2$) ΛN–ΣN system, as already mentioned in the Introduction. This LEC has been set to zero in Ref. [2] because the YN data alone do not allow to establish a value for it. However, as shown in Ref. [3], it can be fixed by considering the Scheerbaum factor S_Λ calculated from the G-matrix, in conjunction with the constraint that the results for ΛN and ΣN scattering remain practically unchanged.

Table 2: Partial-wave contributions to the Scheerbaum factor S_Λ (in MeV fm^5) at $k_F = 1.35$ fm^{-1} for the LO and NLO interactions for various cutoffs. NLO†(650) are results based on the interaction as published in Ref. [2], i.e. without an antisymmetric spin-orbit force.

	${}^3P_0$	${}^3D_1$	${}^3P_1$	${}^1P_1 \leftrightarrow {}^3P_1$	${}^3P_2$	${}^3D_2$	${}^3D_3$	Total
LO (550)	8.7	−0.2	−5.2	0.0	−0.9	0.4	−0.1	2.7
LO (600)	9.3	−0.2	−5.0	0.0	−1.1	0.4	−0.1	3.3
LO (650)	9.8	−0.2	−4.8	0.0	−1.2	0.4	−0.1	3.8
LO (700)	10.4	−0.2	−4.7	0.0	−1.4	0.4	−0.1	4.4
NLO (500)	−5.9	−0.6	−3.3	8.9	−3.4	0.4	0.2	−3.7
NLO (550)	−5.2	−0.6	−2.8	7.5	−3.1	0.4	0.2	−3.7
NLO (600)	−4.8	−0.6	−2.4	6.6	−3.0	0.4	0.2	−3.7
NLO (650)	−4.4	−0.6	−2.0	5.8	−3.0	0.4	0.2	−3.7
NLO†(650) [2]	−4.4	−0.6	−4.6	0.0	−3.0	0.4	0.2	−12.0
Jülich '04 [16]	4.0	0.5	−1.3	4.6	−9.2	0.6	−1.0	−1.7
Jülich '94 [20]	−3.3	1.2	−3.8	8.4	−2.5	0.6	−1.3	−0.4

As guideline for the strength of the Λ-nucleus spin-orbit potential "empirical" values from studies of the splitting of the $5/2$ and $3/2$ states of ${}^9_\Lambda$Be by Hiyama et al. [25] and Fujiwara et al. [26] are used [3]. The results of those authors suggest that values for S_Λ in the order of -4.6 to -3.0 MeV fm^5 would be needed to reproduce the experimentally observed small level splitting [27]. Values of around -3.2 and -4.1 MeV fm^5 are advocated in Refs. [28] and [29], respectively. Since the precise value required for the Λ s.p. spin-orbit strength can only be pinned down reliably via a dedicated calculation of finite hypernuclei based on our EFT interactions, we decided to aim

at an exemplary result of -3.7 MeV fm^5. As one can see in Table 2, this goal can be achieved. For comparison we provide also a prediction based on the original YN of Ref. [2], where there is no antisymmetric spin-orbit force, cf. NLO†(650) in Table 2. In this case S_Λ is roughly a factor four larger and, thus, not in line with the "empirical" information anymore.

5. Summary

We presented results for the in-medium properties of a hyperon-nucleon (YN) interaction derived within chiral effective field theory (EFT) and fitted to ΛN and ΣN scattering data. The single-particle potentials for the Λ and Σ hyperons in nuclear matter were evaluated in a conventional G-matrix calculation, and the Scheerbaum factor associated with the Λ-nucleus spin-orbit interaction was computed.

The predictions for the Λ single-particle potential are found to be in good qualitative agreement with the empirical values inferred from hypernuclear data. A depth of about -25 MeV is predicted by the NLO interaction and of about -36 MeV by the LO potential. The Σ-nuclear potential turns out to be repulsive, in agreement with phenomenological information, with values around 15–20 MeV.

Empirical information suggests that the Λ-nucleus spin-orbit interaction should be rather weak. Therefore, we investigated also the spin-orbit interaction and, in particular, the role of the antisymmetric spin-orbit force in the YN system. In chiral EFT a contact term representing an antisymmetric spin-orbit force arises at NLO which induces $^1P_1$–$^3P_1$ transitions in the coupled ($I = 1/2$) ΛN–ΣN system. However, the low-energy constant associated with the contact term can not be pinned down by a fit to the existing ΛN and ΣN scattering data. Interestingly, it turned out that its value can be indeed fixed from investigating the properties of the Λ hyperon in nuclear matter and, specifically, this low-energy constant can be utilized to achieve a weak Λ-nuclear spin-orbit potential.

Acknowledgements

I would like to thank N. Kaiser, U.-G. Meißner, A. Nogga, S. Petschauer, and W. Weise for collaborating on the topics covered by my talk. Work supported in part by DFG and NSFC (CRC 110).

References

[1] S. Weinberg, Phys. Lett. B **251**, 288 (1990).

[2] J. Haidenbauer, S. Petschauer, N. Kaiser, U.-G. Meißner, A. Nogga, W. Weise, Nucl. Phys. A **915**, 24 (2013).

[3] J. Haidenbauer, U.-G. Meißner, Nucl. Phys. A **936**, 29 (2015).

[4] S. Petschauer, J. Haidenbauer, N. Kaiser, U.-G. Meißner, W. Weise, Eur. Phys.J. A **52**, 15 (2016).

[5] R. R. Scheerbaum, Nucl. Phys. A **257**, 77 (1976).

[6] E. Friedman, A. Gal, Phys. Rept. **452**, 89 (2007).

[7] T. Rijken, M. Nagels, Y. Yamamoto, Nucl. Phys. A **835**, 160 (2010).

[8] O. Hashimoto, H. Tamura, Prog. Part. Nucl. Phys. **57**, 564 (2006).

[9] A. Gal, Prog. Theor. Phys. Suppl. **186** (2010) 270.

[10] E. Botta, T. Bressani, G. Garbarino, Eur. Phys. J. A **48**, 41 (2012).

[11] H. Polinder, J. Haidenbauer, U.-G. Meißner, Nucl. Phys. A **779**, 244 (2006).

[12] J. Haidenbauer, U.-G. Meißner, A. Nogga, H. Polinder, Lect. Notes Phys. **724**, 113 (2007).

[13] S. Petschauer, N. Kaiser, Nucl. Phys. A **916**, 1 (2013).

[14] C.M. Vincent, S.C. Phatak, Phys. Rev. C **10**, 391 (1974).

[15] E. Epelbaum, W. Glöckle, U.-G. Meißner, Nucl. Phys. A **747**, 362 (2005).

[16] J. Haidenbauer, U.-G. Meißner, Phys. Rev. C **72** 044005 (2005).

[17] A. Nogga, Few Body Syst. **55**, 757 (2014).

[18] B.D. Day, Rev. Mod. Phys. **39**, 719 (1967).

[19] Y. Fujiwara, M. Kohno, T. Fujita, C. Nakamoto, Y. Suzuki, Nucl. Phys. A **674**, 493 (2000).

[20] A. Reuber, K. Holinde, J. Speth, Nucl. Phys. A **570**, 543 (1994).

[21] D.J. Millener, C.B. Dover, A. Gal, Phys. Rev. C **38**, 2700 (1988).

[22] M. Kohno, Y. Fujiwara, Y. Watanabe, K. Ogata, M. Kawai, Phys. Rev. C **74**, 064613 (2006).

[23] J. Dabrowski, J. Rozynek, Phys. Rev. C **78**, 037601 (2008).

[24] S. R. Beane *et al.*, Phys. Rev. Lett. **109**, 172001 (2012).

[25] E. Hiyama, M. Kamimura, T. Motoba, T. Yamada, Y. Yamamoto, Phys. Rev. Lett. **85**, 70 (2000).

[26] Y. Fujiwara, M. Kohno, K. Miyagawa, Y. Suzuki, Phys. Rev. C **70**, 047002 (2004).

[27] M. Kohno, private communication.

[28] M. Kohno, Phys. Rev. C **81**, 014003 (2010).

[29] Y. Fujiwara, M. Kohno, Y. Suzuki, Mod. Phys. Lett. A **24**, 1031 (2009).